PHYSICAL REVIEW B VOLUME 13, NUMBER 4 15 FEBRUARY 1976

Intermolecular bonding and lattice dynamics of Se and Te

Richard M. Martin* and G. Lucovsky
Xerox Palo Alto Research Center, Palo Alto, California 94304

K. Helliwell
Physics Department, Arizona State University, Tempe, Arizona 85281
(Received 14 July 1975)

Vibrational modes of trigonal Se and Te are analyzed to determine the character of the interchain (secondary) forces. The dispersion of low-frequency modes clearly demonstrates the directional (covalent) character of these forces. The interference of secondary interactions with the intrachain (primary) bonding is evidenced by the anomalous softening of the zone-center A_1 mode relative to other modes and to corresponding modes in other molecular forms of these elements. The nature of and trends in the forces are consistent with electronic calculations and may be interpreted as aspects of a metal-insulator transition.

I. INTRODUCTION

Understanding of chemical bonding is greatly facilitated by construction of continuous scales which characterize the gradual change of bonding from one type to another. An example is ionicity,[1,2] which quantifies the essentially continuous gradation of binary compounds from purely covalent to ionic bonding. In this paper we explore aspects of chemical bonding associated with the existence of identifiable "molecular" units in condensed matter. The characteristic feature of a molecular material[3] is that groups of atoms are associated into units or molecules with strong internal bonding and only weaker bonding between atoms on different molecules. We shall refer to intramolecular bonding as *primary* and intermolecular bonding as *secondary*. Here we are interested in groups of materials in which the ratio of the secondary to primary bond strengths can be varied from near zero to unity, at which point the distinction between primary and secondary is lost and the material has no molecular character.

The examples considered in the present paper are the various forms of Se and Te. Together with S and Po, these elements from the sixth column of the periodic table span the range from molecular to nonmolecular crystals. All forms of S, Se, and Te under ordinary conditions are molecular in nature, but, as we shall show, with varying degrees of secondary interactions. The molecular units are characterized by strong covalent primary interactions. On the other hand, Se and Te at high pressures[4,5] and Po at zero pressure[6] are stable in metallic nonmolecular forms, which are simple cubic or slight distortions from it. The structure upon which we focus our attention is the trigonal "chain" form of Se and Te, which can be viewed[7,8] as a continuous distortion from the simple-cubic structure. The distortion is one which makes two of the six neighbors in a simple-cubic lattice closer and the other four more distant. Thus this system of elements having the trigonal or cubic structures provides a possible realization of a continuous or nearly continuous transition from covalent to metallic bonding.

In this paper we study the primary and secondary bonding in trigonal Se and Te by examining in detail the lattice vibrational modes. The magnitudes of various forces related to primary and secondary bonding are determined principally by fitting the measured phonon dispersion curves.[9–18] The nature of the resulting forces and their variation between Se and Te are the basis for our description of the covalent to metallic transition occurring in the sequence from Se to Po. It is illuminating also to compare the vibration frequencies in the trigonal crystals with those in other phases in which the secondary interactions are smaller.

The analysis is aided greatly by considering the relation between the covalent and metallic structures as a displacive phase transition.[19] The order parameter of the transition is the trigonal distortion which is the difference in the separation of the two near neighbors from that of the four second neighbors. One consequence is a "softening" of the lattice vibrational mode associated with this order parameter. The softening may be effected either by compositional variation, e.g., in comparing[17] Se and Te, or by pressure. Indeed, anomalous variation in the "soft" mode with pressure is evident in the measurements of Richter *et al.*[20] The use of the order parameter as the relevant variable relates the compositional and pressure variations.[21] Here we do not consider explicitly variations with pressure. However, we require our force models to be qualitatively consistent with the effects of pressure and further considerations are given elsewhere.[21,22]

In Sec. II we describe the various structures in

which Se and Te form. The primary and secondary bonding and the valence-force-field (VFF) model which describes the harmonic forces resulting from the directional bonding is discussed in Sec. III. A convenient method for numerical calculation of the vibrational frequencies from complex VFF models is described in Sec. IV along with a procedure for numerical calculation of algebraic expressions for phonon frequencies at high-symmetry points. The resulting expressions and dispersion curves for trigonal Se and Te are also given in Sec. IV. We discuss the relative importance of the different directional forces for particular vibrational modes and the variations in these forces between Se and Te. Vibrational modes of different forms of Se and Te are discussed in less detail in Sec. V. Certain modes of rings and chains are shown to be closely related and a comparison of these modes is used to determine the interaction constant needed in Sec. IV. Applications are discussed to amorphous Se and Te, which are approximated by molecular units with weak secondary interactions.

II. STRUCTURES

The two "molecular" units from which the stable low-pressure phases[6,23] of Se and Te are formed are the eight-member ring and the infinite spiral chain shown in Fig. 1. The chain is periodic with

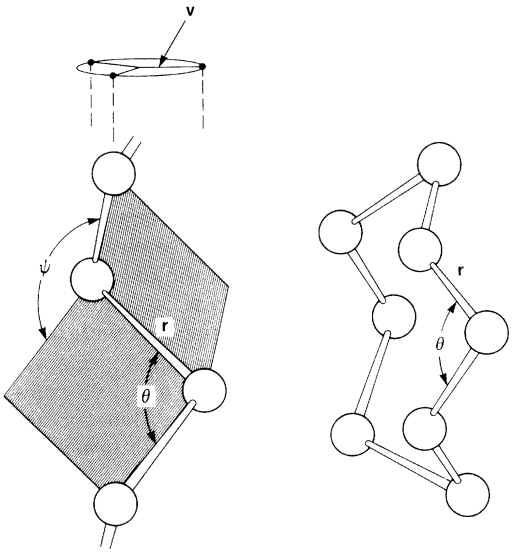

FIG. 1. Local coordination of atoms in the ring and chain forms of Se. The chain form on the left is a helix with a basis of three atoms. The bond length is r, bond angle θ, and the dihedral angle between bonding planes is ψ. The projection of the helix onto the basal plane is shown above where v is the radius of the helix. The eight-member ring is shown at right in a perspective to emphasize the similarity to the chain.

TABLE I. Lattice parameters of crystalline Se and Te taken from Ref. 23. The symbols are explained in the text.

	Se (α-mono)	Se (trig)	Te (trig)
r	~2.32 Å	2.373 Å	2.835 Å
θ	~105.9°	103.1°	103.2°
ψ	~101.0°	100.6°	100.7°
c	···	4.954	5.929
v	···	0.984	1.174
a	···	4.366	4.457
R	~3.58+	3.436	3.495
x	···	0.2254	0.2633
c/a	···	1.135	1.330

a three atom unit cell and has trigonal symmetry about the chain axis. It is either right handed or left handed, depending upon the sense of the spiral. Each atom has two near neighbors at distance r with an angle θ between the bond vectors. The positions of all atoms are fixed by the symmetry and these two parameters. Convenient other parameters uniquely related to these are the lattice constant c, the radius of the spiral shown in the figure as v, and the dihedral angle ψ between adjacent bonding planes. The parameters[23] for chains in trigonal Se and Te are given in Table I.

The eight-member puckered ring molecule is also shown in Fig. 1 from a perspective that shows the similarity to the chain. It is in essence a bent chain in which the sign of the dihedral angle ψ alternates. The magnitude of ψ is constrained as a function of bond length r and angle θ so that the "bent chain" closes with eight atoms. Average values of r, θ, and ψ for the slightly distorted rings in α-monoclinic Se[23] are given in Table I. The similarity between bond lengths and angles and even the dihedral angle in rings and chains is evident; hence we expect the primary bonding (intra-ring or intrachain) to be almost identical. In the case of Te only the chain form is known and no ring molecules have been identified.

A variety of different crystals[6,23] are formed from the ring molecules of Se. We shall not be concerned with the complex packing in these crystals except to note that packing of rings is inefficient compared to chains and hence secondary (inter-ring) bonding is weaker. A typical inter-ring distance is given in Table I. We note that in each crystal known there is at least one shorter intermolecular distance, but none as short as in the trigonal form. Because of the complexity of the secondary interactions and the fact that they must be weaker than in the trigonal case, we shall ignore all secondary interactions in the ring-structured forms.

The modes of vibration of the eight-member ring have been tabulated by Scott *et al.*[24] who give dia-

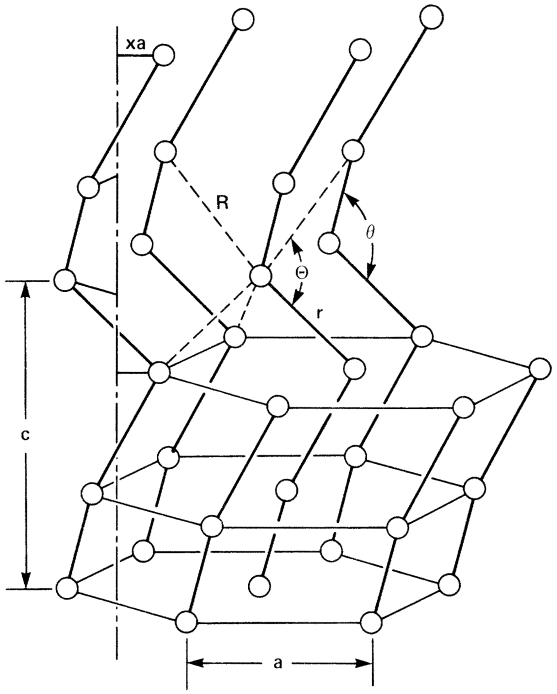

FIG. 2. Schematic illustration of the trigonal lattice structure of Se and Te. Heavy lines denote the chains which spiral about a vertical axis as shown for the chain at the left. The hexagonal packing of the chains is evident in the figure and a and c are the lattice constants. The chain radius, denoted as v in Fig. 1, is defined as xa. Each atom has two first neighbors at distance r and four second neighbors at distance R. The approximate octahedral environment is shown for one atom.

grams for each displacement pattern. One of the symmetric modes is discussed in Sec. V, where we compare ring and chain vibration frequencies.

The trigonal crystalline form of Se and Te is an array of parallel chains arranged on a two-dimensional hexagonal lattice,[6,23] as is illustrated in Fig. 2. The packing of the chains is determined by the lattice constant a in the basal plane relative to the chain radius v. The ratio $v/a \equiv x$ is the usual lattice parameter used to specify the structure. The heavy lines in Fig. 2 designate the primary bonds in the chains. In the crystal each atom also has four equivalent second neighbors at distance R, all on other chains. The four neighbors for one atom are indicated in Fig. 2. As is evident in the figure, the four second neighbors roughly complete a distorted octahedron, i.e., there is one second neighbor approximately opposite each first neighbor and two second neighbors oriented approximately perpendicular to the plane formed by primary bond vectors. The structural information for Se and Te is listed in Table I.

In Table II we list the ratio R/r for the forms of Se and Te so far considered. We see that the ratio decreases significantly in going from the ring to chain form of Se. The ratio decreases even further for Te. We interpret this to imply stronger secondary interactions in the chain form. In fact, as suggested by von Hippel,[8] it appears that secondary interactions are responsible for the increasing stability of the chain versus ring form for the heavier elements. Unlike the ring, the chain is not a stable isolated molecular species; hence we conclude that secondary interactions are essential for the *existence* of the chain. The trigonal structure tends to stabilize the chain form because it allows the four second neighbors at approximately octahedral sites. Later we shall discuss the bonding pictures which qualitatively describe the preference for this geometrical arrangement.

Also given in Table II are the observed bond lengths r and R compared to normal covalent ($2r_c$) and van der Waals ($2R_v$) interatomic distances.[1] We see from these comparisons that secondary interactions are increased, i.e., bond lengths R are decreased from those characteristic of van der Waals bonding. Furthermore there are small increases in the primary bond lengths r over the normal covalent distances in the trigonal crystals. Thus increasing secondary interactions are coupled with decreased primary bond strengths. This is the principal structural evidence for the interaction between primary and secondary bonds discussed below and used in our interpretation of lattice vibrational properties in Secs. IV and V.

Let us now consider the trigonal structure as a function of the free lattice parameter x. The interesting range of x is $x \leq \frac{1}{3}$. At $x = \frac{1}{3}$ the structure ceases to be trigonal and is simple hexagonal. At this point $R = r$ and each atom has six equivalent neighbors. Furthermore we note that for a particular value of c/a ($\sqrt{\frac{3}{2}} = 1.225$) the hexagonal struc-

TABLE II. Relative distances in column-VI elements. The ratio of second- to first-neighbor distances R/r is a measure the molecular nature. In the trigonal crystals it measures the trigonal distortion [Eq. (1)]. The second and third columns list the deviations from ideal covalent and van der Waals radii (taken from Ref. 1, pp. 255 and 260). The deviations are quite large in the trigonal crystals indicating large secondary interactions. Distances in the amorphous form are taken from the x-ray scattering data of Refs. 44 and 46.

	R/r	$r/2r_c$	$R/2R_v$
α-mono. Se	~1.54+	0.99	0.90
Trig. Se	1.45	1.01	0.86
Trig. Te	1.21	1.03	0.79
amorph. Se	1.60	1.0	0.9
amorph. Te	1.52	1.0	1.05
Po	1.00	...	...

ture becomes simple cubic with the c axis of the hexagonal structure becoming the body diagonal in the simple cubic. Thus the free parameters of the trigonal structure x and c/a can be continuously varied to give a hexagonal structure in which each atom is sixfold coordinated, a special case of which is the simple cubic. We note that the transition to sixfold coordination can be realized in practice by the application of pressure.[4,5]

The consequences of the existence of the phase transition are most easily discussed using the general properties near displacive transitions.[19] The transition is describable in terms of an order parameter which must be a linear combination of $x-\frac{1}{3}$ and $c/a-\sqrt{\frac{3}{2}}$, since these fully describe the trigonal distortion. We choose as our parameter $R/r-1$ because this is the dimensionless quantity most closely related to chemical bonding—i.e., distances between atoms—and because it is the appropriate parameter at large distortions. Note that for small values of the order parameter, $R/r-1 \ll 1$, we have

$$R/r-1 \approx (x-\tfrac{1}{3})\{\tfrac{3}{2}/[1+\tfrac{2}{9}(c/a)]\}. \quad (1)$$

Thus to linear order, the chosen order parameter is directly proportional to $x-\frac{1}{3}$ and is independent of $c/a-\sqrt{\frac{3}{2}}$. Our physically motivated choice of the order parameter therefore is relevant for consideration of the trigonal $\rightarrow$ hexagonal transition and any subtleties associated with the purely elastic hexagonal-cubic transition are ignored.

An immediate consequence of the identification of the order parameter is that the dynamical mode associated with the order parameter is predicted to soften as the transition is approached. As discussed later in Sec. IV, it is the Γ_1 optic mode (termed A_1) which is directly related to the order parameter $x-\frac{1}{3}$; hence, this is the mode which is expected to vary anomalously. Even far from the transition (e.g. at zero pressure) we can expect the A_1 frequency to be depressed. Anomalies in the A_1 frequencies have already been pointed out (i) by comparing[17] measured frequencies in Se and Te and (ii) by observation of a rapid decrease in the A_1 frequency under pressure.[20] To analyze this behavior we next consider models of the bonding, which suggest driving forces for the "softening" of the A_1 mode as well as related aspects of the directional forces. In Sec. IV we describe in detail the relation of these forces to the A_1 optic mode frequency.

We also note that other physical properties are expected to be simply related to the order parameter. One is optical activity which may be nonzero in the trigonal crystal but must vanish in the hexagonal one.[25] The activity results from the "handedness" of the chains, a property which clearly vanishes as one approaches the symmetric hexagonal structure where the chains themselves lose their identity. Another property is the quadrupole field at each nucleus.[26] This is exactly zero in the cubic form but is nonzero in the hexagonal symmetry. At the hexagonal $\rightarrow$ trigonal transition, an anisotropy in the field about each nucleus develops in the basal plane. The magnitude of the quadrupolar fields have been investigated in both Se and Te.[27]

Finally, it is interesting to note that other systems have similar structural characteristics and order parameters. An example is the elements in column V of the periodic table. The elements have a tendency toward threefold coordination, which leads to stable structures that are continuous distortions from the simple-cubic lattice.[6]

III. BONDING AND THE FORCE MODEL

We now consider the bonding in these materials and utilize an atomic-orbital picture[28] of the valence states for a qualitative description of the forces. The relevant atomic states are the outer s and p orbitals of each element, respectively, with the eight states partially filled by six electrons. The traditional picture[28-30] of the primary bonding within a ring or chain is illustrated in Fig. 3. It is assumed that two hybridized orbitals h_1 and h_2

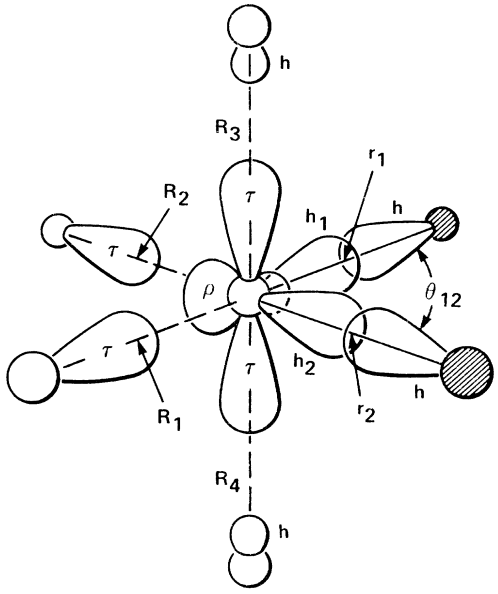

FIG. 3. Bonding in trigonal Se and Te. The h orbitals are bonding orbitals hybridized from s and p atomic orbitals; the τ orbitals are the p-like nonbonding states; and the ρ orbital is the primarily s nonbonding state. Also shown are τ orbitals on atoms on neighboring chains which overlap bonding and antibonding states to produce secondary (interchain) bonding. The notation r_1, r_2, θ_{12} is used to denote the general valence force field coordinates for any triad of atoms.

are formed with lobes pointing toward the two near neighbors shown shaded in Fig. 3. These combine with like orbitals from the neighbors to form the two bonding states about each atom. These states require two electrons per atom. The remaining four electrons fill nonbonding states, ρ and τ, on each atom. The τ state is simply the p state perpendicular to the bonding plane and is not mixed with the other atomic states by the presence of the nearest neighbors. The ρ nonbonding state is primarily s-like and its mixing with bonding states is determined by the nearest-neighbor interactions. The τ nonbonding pair state is highest in energy, the bonding combination of the h states is intermediate, and the s-like ρ nonbonding pair forms the lowest energy valence states in the ring or chain.[29,30]

The equilibrium values of the bond lengths r and angles θ are determined by maximizing the bonding energies, i.e., by optimizing the overlap of the h bonding states which are hybridized combinations of s, p, and possibly[30] d atomic states. Deviations from the equilibrium lengths or angles require readjustment of the bonding functions causing both angular and radial restoring forces. This is most naturally described by writing the total energy of the system in a valence-force-field (VFF) form as a function of the set of all bond lengths $\{r\}$ and angles $\{\theta\}$. The VFF model is described below and is identical to that used by others[33–37] for the primary bonding.

Consider now the secondary (interchain) interactions in the trigonal crystal, which we argue must be treated in a way similar to the primary bonds. We recall the second neighbors roughly complete an octahedron about each atom (see Fig. 2). These four neighbors are shown as open circles in Fig. 3 and relevant orbitals on them are shown. We see that the trigonal crystal forms so that each nonbonding τ orbital overlaps the ρ and the back lobes of the bonding orbitals on atoms on adjacent chains. Krebs[28] shows the overlap explicitly for atomiclike functions, and suggests it is strong enough to interfere with the primary bonding, i.e., a resonance[1] or mesomeric[28] interaction. It is the overlap of filled states that provides the repulsion that stabilizes the crystal, but at the same time overlap of the τ orbitals with unfilled *antibonding* states on different chains tends to *interfere* with primary bonds. The interactions with unfilled states always lowers the energy of the filled states, in this case by forming secondary bonds at the expense of primary bonds. The mixing of primary and secondary bonding shows that secondary bonds (a) develop covalent character and (b) weaken primary bonds. In the limit $R = r$ the two types of bonds are indistinguishable and only partially filled, i.e., the crystal is a metal.

The pseudopotential-band-structure calculations of Joannopoulos *et al.*,[30] which are fitted to empirical electronic density of states, show clearly the effects of secondary interactions. Their calculated charge densities as a function of separation between the chains show an increased secondary and decreased primary bonding charge as the chains are brought together. They have also fitted tight-binding electronic parameters to the band structure and find the largest secondary matrix elements to be those between lone pair τ and both bonding and antibonding states on neighboring chains. The ratios of the largest secondary to primary bonding matrix elements is ~ 0.2 and ~ 0.5, respectively, for Se and Te. These arguments together with the structural information discussed in Sec. II shows that secondary bonds should be treated in a way comparable to that for primary bonds, i.e., also in a VFF model.

The resulting VFF expression for the lattice energy to harmonic order has the form

$$U = \sum \{\tfrac{1}{2}K_r(\Delta r)^2 + \tfrac{1}{2}K_\theta(r\Delta\theta)^2 + K_{rr'}\Delta r\Delta r' + K_{r\theta}\Delta r(r\Delta\theta) + \tfrac{1}{2}K_R(\Delta R)^2 + \tfrac{1}{2}K_\Theta[(rR)^{1/2}\Delta\Theta]^2 + K_{R\Theta}\Delta R[(rR)^{1/2}\Delta\Theta] + K_{rR}\Delta r\Delta R\}. \quad (2)$$

The first four terms are the primary (intrachain) interactions, where K_r is the central bond-stretching force constant, K_Θ is the angular constant, and $K_{rr'}$ and $K_{r\Theta}$ are cross terms that couple neighboring bond lengths and an angle with the length of each constituent bond. The fifth term involving K_R is the secondary (interchain) bond-stretching force constant. All these five terms are exactly the same as have been considered previously.[33–37]

The final three terms are the directional three-body interchain forces which have not been considered in previous work. Here Θ denotes an angle between a primary and a secondary bond vector as illustrated in Fig. 2. The $K_{R\Theta}$ term couples an angle with the length of second-neighbor bond that joins a leg of the given angle. We have omitted the $\Delta r[(rR)^{1/2}\Delta\Theta]$ term in Eq. (2) because it can easily be shown that it only makes negligible contributions to the high-frequency modes. Simple considerations show that K_Θ and $K_{R\Theta}$ become meaningless for $\Theta \to 180°$, and we choose to consider only the $\sim 90°$ angles (see Fig. 2) and to set K_Θ and $K_{R\Theta}$ the same for each of the six $\sim 90°$ angles Θ about each atom although these constants are not strictly equivalent by symmetry. Wendel *et al.*[38] have independently used forces of a very similar form to describe the secondary forces in Se.

The final term involving K_{rR} in Eq. (2) couples primary and secondary bond lengths. The bonding arguments above suggest that such a term results from the competition of primary and secondary

bonding mechanisms. For simplicity we treat all K_{rR} interactions as equal and the sum in (5) is over all eight pairs of first and second neighbors about each atom. If K_{rR} is positive, it depresses the frequency of any mode in which the average Δr is opposite in sign to the average ΔR. This is the driving force toward a more symmetric (less distorted) trigonal structure. We shall see explicitly in the following section the lowering of the A_1 mode caused by $K_{rR}>0$.

For large secondary bonding there are additional secondary terms such as the final one in Eq. (2), where $K_{RR'}$ is the constant which couples the two oppositely directed second-neighbor bonds about each atom. This term is included in the algebraic formulas of Sec IV, but its effect is small in the cases considered and $K_{RR'}$ is omitted in our calculations.

Also there are long-range forces which are entirely neglected in the present work. Each Se or Te has a dipole moment in the trigonal structure. Displacement of and changes in the dipoles with atomic displacements contribute to the restoring forces. It is shown in Ref. 38 that such long range forces can affect significantly the dispersion in the upper optic modes. Also macroscopic electric fields are generated for certain modes.[38-40] We omit all long-range forces and explore only the short-range chemical bonding. Of course, we therefore have no macroscopic electric fields and consequently cannot describe the longitudinal-transverse splittings and infrared activity allowed in the trigonal crystal.[38-40]

IV. CALCULATION OF PHONON DISPERSION CURVES

The dynamical matrix for the phonons of wave vector q is defined by[41]

$$D_{ij}^{\alpha\beta}(\vec{q})=\frac{1}{2N}\frac{1}{(M_iM_j)^{1/2}}\sum_{l'l''}\left(-\frac{\partial^2U}{\partial R_{l'i}^{\alpha}\partial R_{l''j}^{\beta}}\right)\times e^{i\vec{q}\cdot(\vec{R}_{l'i}-\vec{R}_{l''j})}. \tag{3}$$

Here U is the internal energy, N is the number of unit cells, α, β are Cartesian coordinate indices, l' and l'' label the unit cells, and i and $j=1, \ldots,$ n denote atoms in the unit cell of mass M_i and M_j, position $\vec{R}_{l'i}$ and $\vec{R}_{l''j}$. The eigenvalues and eigenvectors of the dynamical matrix are the squared phonon frequencies and the normal mode displacements given by

$$D(\vec{q})\lambda_r=\omega_r^2\lambda_r, \quad r=1,3n. \tag{4}$$

Here we have omitted the indices on the dynamical matrix and eigenvectors λ_r for simplicity.

The novel aspect of our approach is in dealing with complicated sets of three-body forces in U, e.g., those in Eq. (2). Inclusion of many such forces is tedious unless done in a general manner. The complication is that each derivative $\partial^2U/\partial\vec{R}_{l'i}\partial\vec{R}_{l''j}$ in Eq. (3) may depend upon many three-body interactions involving atoms $l'i$, $l''j$, and all possible other atoms as the third atom. To carry out the computations it is much more convenient to reorder the summations needed in (3). We note that U is a sum of three-body terms (ignoring two-body terms for the moment)

$$U=\sum_{l,k}\sum_{s,s'}U_{lk}^{ss'}, \tag{5}$$

where $U_{l,k}^{ss'}$ denotes a three-body interaction in which atom lk is the central atom and s and s' are a compact notation for atoms l_sk_s and $l_{s'}k_{s'}$, two different neighbors of atom lk. Inserting Eq. (5) in Eq. (3) and using translation invariance, we find

$$D_{ij}^{\alpha\beta}(\vec{q})=\frac{1}{2(M_iM_j)^{1/2}}\sum_{kss'}\left(\sum_{l'l''}-\frac{\partial^2U_{0k}^{ss'}}{\partial R_{l'i}^{\alpha}\partial R_{l''j}^{\beta}}\,e^{i\vec{q}\cdot(\vec{R}_{l'i}-\vec{R}_{l''j})}\right). \tag{6}$$

The advantage now is that the double sum in brackets is readily carried out because $U_{0k}^{ss'}$ involves only the positions of three atoms. The three-body VFF terms for a triad of atoms with bond lengths r_1 and r_2 and include angle θ_{12} can be written in general

$$U=\tfrac{1}{2}K_{\theta_{12}}(\bar{r}\Delta\theta_{12})^2+K_{r_1\theta_{12}}\Delta r_1(\bar{r}\Delta\theta_{12})+K_{r_2\theta_{12}}\Delta r_2(\bar{r}\Delta\theta_{12})+K_{r_1r_2}\Delta r_1\Delta r_2. \tag{7}$$

An algebraic expression for the bracketed sum in (6) in terms of the general set of three-body constants in Eq. (7) can be given solely in terms of the direction cosines that relate Cartesian displacements to angles and lengths.[31,32]

We have written a computer program which carries out the sum in (6) over atoms in the unit cell k and the double sum over neighbors s and s'. The program finds and orders the neighbors of each atom $0k$. It is then straightforward to define criteria which insert the proper three-body constants into the general expressions for each relevant pair of neighbors. Consider the case described by Eq. (2). When s and s' are the two first neighbors, $K_{r_1r_2}=K_{rr'}$, $K_{r_1\theta_{12}}=K_{r_2\theta_{12}}=K_{r\theta}$, and $K_{\theta_{12}}=K_{\theta}$. For s a first neighbor and s' a second neighbor oriented

at approximately 90°, $K_{r_1r_2}=K_{rR}$, $K_{r_1\theta_{12}}=0$, $K_{r_2\theta}=K_{R\Theta}$, and $K_{\theta_{12}}=K_{\Theta}$. For s a first neighbor and s' a second neighbor oriented at approximately 180°, $K_{r_1r_2}=K_{rR}$, $K_{r_1\theta_{12}}=K_{r_2\theta_{12}}=K_{\theta_{12}}=0$. These completely specify all the three-body contributions to the dynamical matrix. The two-body central forces are easily treated[41] and are added to the three-body contributions to complete the dynamical matrix.

The adjusted dispersion curves are presented later in this section. The direct numerical results, however, are of limited usefulness and we first derive the algebraic forms for the frequencies of certain high symmetry modes. Consider a case in which the modes of a given symmetry are denoted by $r=1,p$. The eigenvectors and eigenvalues in general are functions of the values of the force constants, however, the eigenvectors λ_r, $r=1,p$, for *any* set of force constants form a complete set for this symmetry. They may be used to project out the relevant $p\times p$ part of a general dynamical matrix, and the eigenvalues are the solutions of

$$\left|\langle\lambda_r|D(\vec{q})|\lambda_{r'}\rangle-\omega^2\delta rr'\right|=0\,. \tag{8}$$

The general form of the dynamical matrix is linear in the force constants K_m so the matrix elements in Eq. (8) may be written

$$\langle\lambda_r|D(\vec{q})|\lambda_{r'}\rangle=M^{-1}\langle\lambda_r|\sum_m K_m A_m(\vec{q})|\lambda_{r'}\rangle$$

$$\equiv M^{-1}\sum_m K_m A_{mrr'}\,. \tag{9}$$

Here D and A_m are $3n\times 3n$ matrices with the indices omitted for brevity. In general M is the mass matrix $(M_iM_j)^{1/2}\delta_{\alpha\beta}$, which in the present case is the scalar atomic mass. The dimensionless matrix A_m may be viewed as the dynamical matrix for unit mass and VFF force constant $K_m=1$, with all other force constants equal to zero. Each matrix A_m is independent of the masses and values of the force constants and depends only upon the structure and the definition of the mth constant in the VFF model.

In the present case of trigonal Se and Te there are four points in the Brillouin zone at which the matrix simplifies greatly. These are the center of the zone Γ and the three zone-boundary points Z, B, and M shown in Fig. 4. At each point the dynamical matrix can be block diagonalized into one 1×1, one 2×2, and two 3×3 submatrices, Γ_1, Γ_2, Γ_3; Z_1, Z_2, Z_3; etc. The two 3×3 matrices are degenerate in each case and we need not distinguish between them. Furthermore, at Γ three modes (one Γ_2 and one Γ_3 pair) are zero by translation invariance; hence the nonzero Γ_2 frequency is given by a single equation, and the two nonzero Γ_3 frequencies are given by a 2×2 matrix equation.

The dimensionless coefficients $A_{m,rr'}$ are given in Table III for both Se and Te for each 1×1 and

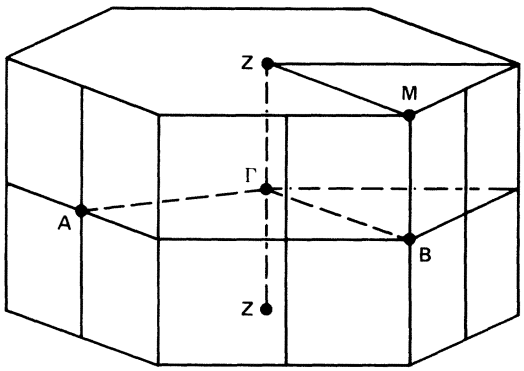

FIG. 4. Brillouin zone in trigonal Se and Te with the high-symmetry points.

two interesting 2×2 cases. In the former case the frequency is given by

$$\sum_m A_m K_m-M\omega^2=0 \tag{10}$$

and in the latter by

$$\left|\begin{bmatrix}\sum_m A_{m,11}K_m-M\omega^2 & \sum_m A_{m,12}K_m\\ \sum_m A^*_{m,12}K_m & \sum_m A_{m,22}K_m-M\omega^2\end{bmatrix}\right|=0. \tag{11}$$

Of course, the 2×2 matrices are not unique and we have chosen as basis vectors the actual eigenvectors in Se and Te, respectively, to show clearly the nature of each mode.

The differences in the coefficients for Se and Te result from geometrical factors, i.e., the differences in c/a and bond angle θ. Since θ is essentially the same in the two materials, the coefficients in Table III may be approximated as a function of c/a. Expressions for the phonon frequencies at different c/a (for example, under pressure) can be derived by interpolation using the coefficients in Table III.

The nature of each mode considered can be directly extracted from Table III. Consider the modes at Γ for which diagrams of the motion are given in Fig. 5. The Γ_2 mode (A_2) is a chain rotation mode which is independent of all forces internal to the chains. The Γ_1 mode (A_1) is the chain expansion mode in which each atom moves in the basal plane. It has contributions from both K_r and K_R and since Δr and ΔR are opposite, this mode is decreased by K_{rR}. The fact that K_{rR} has maximum effect on Γ_1 is evident in Table III. The $\Gamma_3(E)$ modes separate into predominantly bond-bending and bond-stretching types with larger admixture in Te. The comparison of Γ_1 and B_1 modes is interesting. The only difference is that at Γ all chains expand in phase, and at B neighboring chains have different phases. This leads to the

TABLE III. Expansion of dynamical matrices for Se and Te for high-symmetry modes. For the five modes fixed by symmetry (Γ_1, Γ_2, B_1, Z_1, M_1) the frequencies are given by $M\omega^2 = \sum_m A_m K_m$ where the coefficients A_m are given in the Table. For the other modes, such as Γ_3 and B_2 given in the Table, the frequencies are the solutions of the 2×2 determinant, Eq. (11).

		K_r	$K_{rr'}$	$K_{r\theta}$	K_θ	K_R	$K_{RR'}$	$K_{R\theta}$	K_θ	K_{rR}
Se	Γ_1	1.55	3.10	−9.23	3.44	2.19	2.19	3.42	2.73	−20.84
	Γ_2	0	0	0	0	2.42	−2.42	−24.96	24.06	0
	Γ_3 11	0	0	0.14	4.75	3.16	−3.16	−21.16	13.04	0.14
	Γ_3 22	2.23	−2.23	−1.37	0.21	0.54	0.54	−3.93	15.38	1.26
	Γ_3 12	−0.05	0.05	−3.23	1.00	0.12	−0.14	2.95	−7.02	−3.28
	B_1	1.55	3.10	−9.23	3.44	1.15	1.15	−1.95	7.23	−5.21
	B_2 11	0	0	0	0	0.10	−0.10	0.89	11.67	0
	B_2 22	0	0	0	0	2.43	−2.43	−12.10	10.44	0
	B_2 12	0	0	0	0	−0.51	0.51	−0.94	6.55	0
	Z_1	0	0	0	1.63	0.81	0.81	−3.11	3.05	0
	M_1	0	0	0	1.63	1.84	1.84	3.19	5.96	0
Te	Γ_1	1.54	3.08	−9.24	3.46	1.64	1.64	5.25	3.14	−18.00
	Γ_2	0	0	0	0	2.44	−2.44	−22.53	20.24	0
	Γ_3 11	0.11	−0.11	−1.50	4.95	2.92	−2.85	−15.96	7.78	−1.31
	Γ_3 22	2.12	−2.12	0.28	0.01	1.03	0.36	−8.58	17.97	3.76
	Γ_3 12	0.49	−0.49	−3.20	−0.21	−0.83	1.15	6.95	−4.72	−2.39
	B_1	1.54	3.08	−9.24	3.46	1.02	1.02	−1.53	7.39	−4.50
	B_2 11	0	0	0	0	0.06	−0.06	0.86	12.23	0
	B_2 22	0	0	0	0	2.88	−2.88	−11.14	7.40	0
	B_2 12	0	0	0	0	−0.40	0.40	−2.26	5.14	0
	Z_1	0	0	0	1.63	0.81	0.81	−3.06	2.02	0
	M_1	0	0	0	1.63	1.43	1.43	4.15	6.18	0

fact that the B_1 mode has a smaller dependence upon K_R and K_{rR}.

The lower B_2 mode is of particular interest. If there were no noncentral secondary interactions, i.e., $K_\Theta = K_{R\Theta} = 0$, the frequency of this mode would be zero.[34] This is essentially a screw mode of the chains in which no second-neighbor distances are changed. The frequency is very nearly given by $\omega^2 \propto K_\Theta$. At Z, alternate unit cells along the chains are exactly out of phase and M is the corresponding point at which different chains are also out of phase. In these cases the single modes Z_1 and M_1 are low-frequency modes which involve no stretching of primary bonds. These modes, along with B_2 and Γ_2, are particularly relevant for understanding the secondary interactions.

With the above descriptions of the modes it is straightforward to adjust the force constants to fit frequencies measured by neutron scattering and by optical techniques. We have carried out a fitting by crudely adjusting constants to fit relevant data.[42] No least squares or other systematic optimization procedure was used. The resulting dispersion curves are shown in Figs. 6 and 7 for Te and Se respectively. The force constants used are given in Table IV. Calculated and experimental elastic constants are given in Table V.

The procedure which we used to arrive at the force constants is: (i) adjust K_Θ to fit the lower B_2 mode, (ii) K_R to fit the compressibility in the basal plane $C_{11}+C_{12}$, (iii) $K_{R\Theta}$ to fit Γ_2 (this also has an effect upon $C_{12}+C_{12}$), (iv) K_θ to approximately fit C_{33}, Z, and the lower Γ_3 modes, (v) K_r, $K_{rr'}$, and

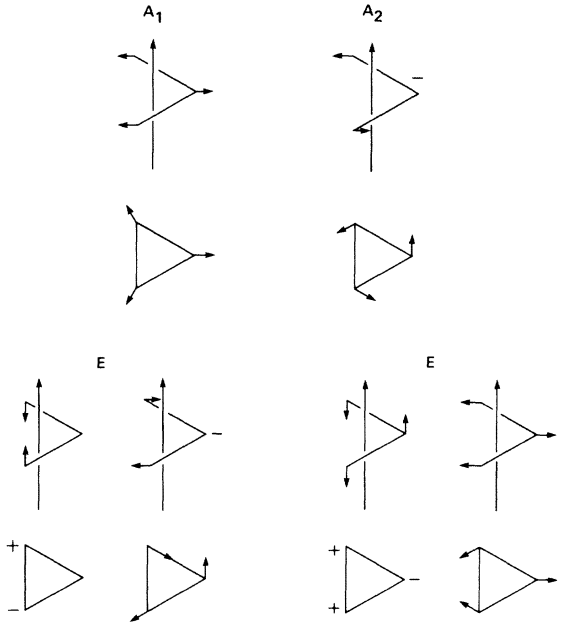

FIG. 5. Displacement pattern for modes at Γ in trigonal Se or Te. The modes are $\Gamma_1(A_1)$, $\Gamma_2(A_2)$, and $\Gamma_3(E)$. In each case views of the displacements are given from beside and from above the chain.

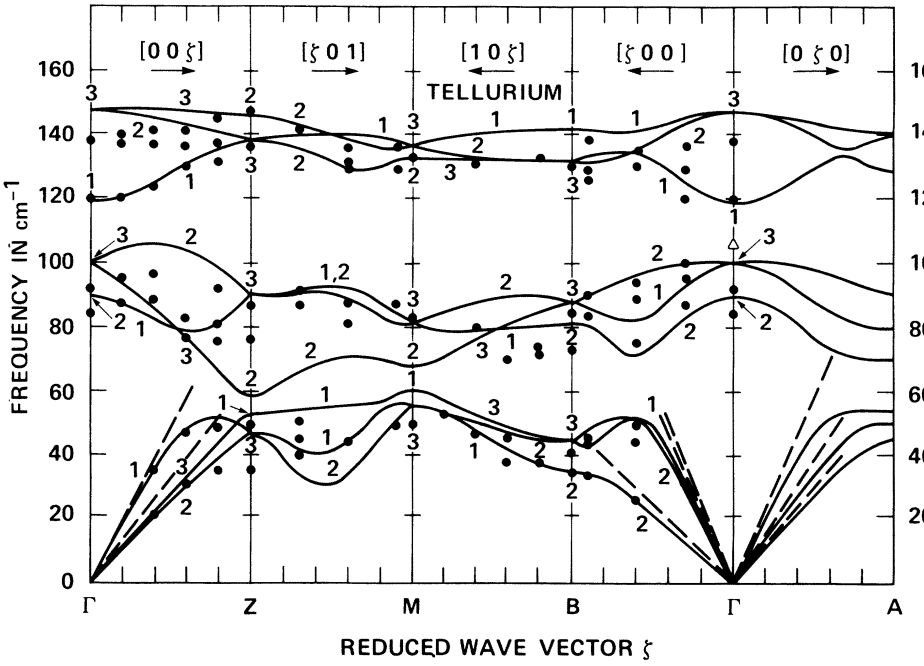

FIG. 6. Phonon dispersion curves of Te. The notation of the symmetry points is given in Fig. 4. Points are experimental data from Ref. 10 and the solid lines are the fitted dispersion curves from the present calculations using the force constants listed in Table IV. The dashed lines result from ultrasonic sound velocities and the calculated and experimental elastic constants are given in Table V. Triangles indicate infrared (Ref. 13) and Raman (Ref. 14) frequencies.

$K_{r\theta}$ to fit Γ_1, the upper Γ_3, and the upper modes at Z. In both cases adjustment (iv) leads to the lower Γ_3 slightly high and C_{33} slightly low. The last adjustment was made very approximately because neutron data on the upper modes in[42] Se became available only after our calculations were complete and because a good fit could not be found for Te. We believe the difficulty in Te results from a need for a more complete description of the primary (intrachain) forces extending to further neighbors. Since this is not the object of the present work, we have not attempted a better description.

Within the limits of our model, we found little improvement for Te by varying $K_{r\theta}$. Thus we set $K_{r\theta}=0$ in both Se and Te. Taking $K_{r\theta}\neq 0$ could improve the agreement at Γ but at the expense of the

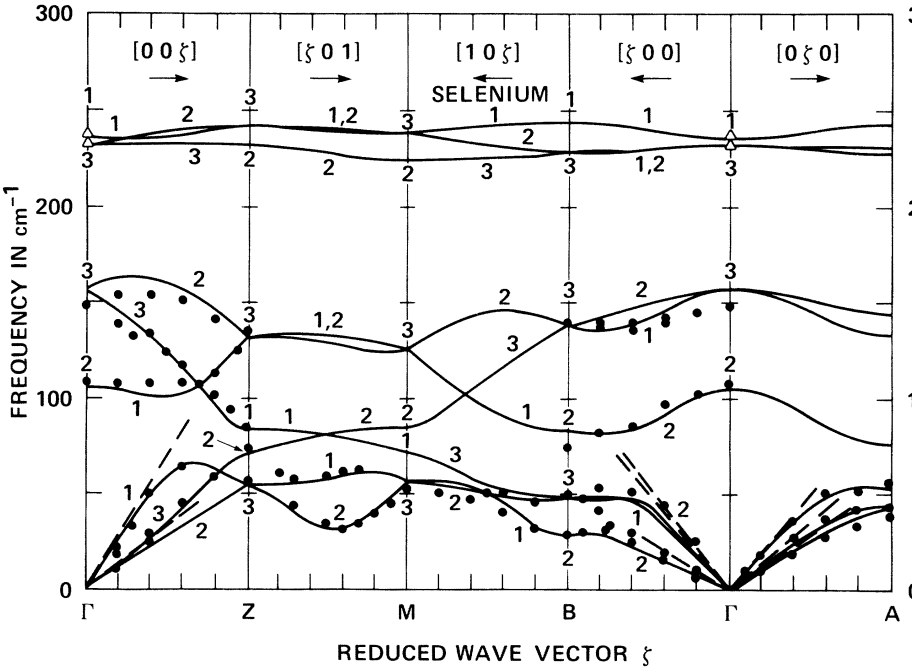

FIG. 7. Phonon dispersion curves of Se. The points are the experimental data from Ref. 11 and the solid lines are the fitted dispersion curves from the present calculations using force constants given in Table IV. The dashed lines result from velocities of sound and the calculated and experimental elastic constants are given in Table V. Triangles indicate infrared (Ref. 13) and Raman (Ref. 15) frequencies.

TABLE IV. Adjusted force constants in Se and Te in units of 10^5 dyn/cm. The notation is discussed in the text preceding Eq. (2). Note that primary forces are large in Se whereas secondary ones are larger in Te.

	Se	Te	K_{Te}/K_{Se}
K_r	1.18	0.66	0.56
$K_{rr'}$	0.13	0.10	0.77
$K_{r\theta}$	0	0	...
K_θ	0.14	0.04	0.29
K_R	0.064	0.13	2.03
$K_{R\Theta}$	−0.011	−0.006	0.55
K_Θ	0.0035	0.0075	2.14
K_{rR}	0.012	0.034	2.83

modes at Z in Te. It is interesting to note that large values of $K_{r\theta}$ were needed in previous calculations[33–37] to fit the low value of the Γ_1 frequency. (This effect is evident in Table III.) In the present case this is accomplished by K_{rR} and $K_{r\theta}$ is not essential.

We have chosen to determine K_{rR} by comparing the Γ_1 mode in the trigonal crystals with modes in other structural modifications as described in Sec. V. In this case the experimental data for Se are best established and we can use accurately known ring and chain frequencies. For Te we compare with the dominant Raman frequency in the amorphous form. We test the choice of K_{rR} by comparing the results for the trigonal crystal with the limited experimental information on the dispersion of the upper optic modes for wave vectors perpendicular to the c axis, in particular, $\Gamma_1 \to B_1$.

We see from the figures that in general, agreement is very good where comparisons with experiment[10–12,42] can be made. Of particular note are the $\Gamma \to B$ and $\Gamma \to Z$ lower dispersion curves. The value of the Γ_2 chain rotation frequency and the downward dispersion from Γ_2 to B_2 in both Se and Te is well described by the inclusion of the noncentral secondary constant $K_{R\Theta}$. In all previous calculations[33–37] with only central secondary forces the B_2 frequency is equal to or greater than the Γ_2 frequency. For Se we find the noncentral forces are the primary restoring forces for the Γ_2 mode. This is in keeping with the result of Nakajama and Odajima,[36] who calculated a frequency of only 49 cm^{-1} compared to the measured value[13] of 103 cm^{-1} for the Γ_2 mode. The other low-frequency modes from Γ to B are also in good agreement supporting our model for the interchain forces.

The lower modes from Γ to Z are given quite accurately in our calculations for Se; in particular the lower Z_2 and Z_3 frequencies agree with experiment and are in the correct order in contrast to the results of Ref. 37. On the other hand there are large discrepancies for Z_1 and the lower Z_2 modes in Te. Similar results are found in other calculations,[10,33,34] including the bond-charge calculations of Cowley.[39] The discrepancies are reduced in the more involved models of Powell and Martel.[10] As mentioned above and as is evident in Fig. 6, the highest optic modes from Γ to Z in Te are also not well described. The experimental results[42] for Se also indicate a much wider upper optic mode bond than we have calculated. We conclude that more complicated intrachain forces beyond the scope of the present work are present in both Se and Te.

The other important feature is the "softening" of the Γ_1 mode. We see from the calculated $\Gamma_1 \to B_1$ dispersion that interaction terms of the form of K_{rR} can have large effects. If K_{rR} were not included we would find the same result as in Refs. 34–37 that the calculated B_1 frequency would be lower than the Γ_1 frequency. The K_{rR} forces clearly improve the agreement with experiment.[10–12] In Te our calculated value for B_1 appears to be somewhat too high whereas in Se the $B_1 - \Gamma_1$ splitting is lower than the experimental value.[42]

Since the anomalous[18] Γ_1 frequencies in Se and Te are here related to secondary forces (K_{rR}) rather than primary forces ($K_{r\theta}$) as considered previously, the present model leads to a natural explanation for the pressure dependence of the Γ_1 frequency. The comparison of force constants in Se and Te shows that as secondary interactions are increased (i.e., as R/r is decreased toward 1) K_R increases, but K_{rR} increases even more rapidly. We expect[21] these trends to hold also as R/r is changed under pressure. Thus it is a natural consequence of the present model of secondary forces that the Γ_1 frequency should decrease rapidly with pressure. All other Γ modes would be expected to have a smaller dependence upon pressure since they are less dependent upon K_{rR}. (See Table III.) This is qualitatively the result found experimentally.[20] A more detailed examination of the Γ modes under pressure is given elsewhere.[21,22]

Directional interchain forces similar to those in

TABLE V. Elastic constants of Se and Te in 10^{10} dyn/cm^2. Experimental values are from Ref. 18.

	Se		Te	
	Expt.	Calc.	Expt.	Calc.
C_{33}	82.0	74.1	70.5	66.4
$\frac{1}{2}(C_{11}+C_{12})$	10.9	11.2	20.5	19.7
$\frac{1}{2}(C_{11}-C_{12})$	8.2	6.8	12.5	10.7
C_{13}	23.0	15.0	23.1	24.4
C_{44}	18.2	14.9	31.9	20.8
C_{14}	6.2	6.7	11.9	9.2

the present work have been proposed independently by Wendel, Weber, and Teuchert for Se.[38] They have included forces associated with the intrachain angle that is ~180° and have set $K_{rR}=0$ for the ~90° angles. Their results are very similar and values of the force constants are quite comparable to those given here. It is of interest that they find an average interaction between first and second neighbor bond lengths to be $K_{rR}=0.02\times10^5$ dyn/cm which is larger than the value of 0.012×10^5 dyn/cm which we derived from the comparison of ring and chain frequencies. This reflects the observation made above that we would have to increase K_{rR} to fit the neutron scattering data of Ref. 12. For the lower frequency modes the most apparent difference of the present results from those of Ref. 38 is the ordering of the lower modes at the M point. No firm conclusion can be drawn from this difference since the frequencies of these modes have not been reported in either of the experimental papers on Se.[11,12] Wendel *et al.*[38] have also carried out shell model calculations which improve the description of the highest optic modes from Γ to Z.

V. RING AND AMORPHOUS FORMS

In this section we discuss aspects of the lattice vibrations in α-monoclinic "ring" Se (α-Se), amorphous Se (a-Se), and amorphous Te (a-Te). Our purpose is to compare with the trigonal crystals and hence we consider only the highest optical frequencies. The lower frequency modes are more affected by geometrical arrangements of the atoms and comparisons are difficult.

The most relevant modes to compare are the high-frequency symmetric Raman-active A_1-type modes of the rings and chains. We have seen in the previous section that this mode is particularly sensitive to the secondary bonding constant K_{rR}. There is no unique relation between the A_1 frequencies of the ring and chain (also termed Γ_1) as is obvious since there are two A_1 modes of the ring. However, for every case we have considered, if we omit secondary interactions and assume the same primary force constants (K_r, $K_{rr'}$, $K_{r\theta}$, and K_θ), the Γ_1 chain mode and upper A_1 ring mode are very close in frequency. We expect changes in primary bonding to be small since the bond lengths and angles are so similar, as listed in Table I. Therefore we attribute any large differences in the A_1 frequencies to secondary interactions.

Experimentally it is found that the A_1 mode in α-Se has frequency[43] 256 cm^{-1} whereas in trigonal Se the A_1 frequency is 237 cm^1. Within any models we have explored, this difference can only be explained by the primary-secondary interaction term K_{rR} described for the trigonal form in Secs. III and IV. We estimate the K_{rR} force constant by the following procedure: (i) We assume each primary constant in the chain is reduced from that in the ring by $(r_{\text{ring}}/r_{\text{chain}})^3=(2.32/2.34)^3=0.975$. (ii) We neglect all secondary interactions for the ring but include the contributions to the A_1 chain frequency from the secondary interactions K_R, $K_{R\Theta}$, and K_Θ. These were all determined from the lower dispersion curves in the trigonal crystal. (iii) Any remaining difference in the A_1 frequencies is attributed to K_{rR} in the trigonal form. From this we calculate the value of K_{rR} for Se given in Table IV and used in the previous section. We have also calculated the other $24-6=18$ modes of a ring and find them to be in reasonable agreement with experiment[24] except for the lowest modes where torsional forces or secondary forces are probably important.

It has been observed that in amorphous a-Se, the Raman spectrum has a large peak near the upper A_1 ring frequency.[15,16] Since it is believed that a-Se is not solely rings, this is interpreted to mean that all molecular species in a-Se have approximately this frequency for the high-frequency symmetric modes. As is evident from our previous discussion, the present calculations indicate that this frequency is not determined by the molecular specie (ring or chain) but by secondary interactions. Therefore we conclude that the geometrical packing of the possible rings and (bent) chains in a-Se is such that all secondary interactions are small. A simple picture of a-Se that derives from these arguments is that of relatively isolated rings and chains. This is supported by experimental radial density distributions[44] of atoms, which indicate (Table II) closer first neighbors and more distant second neighbors in a-Se compared to trigonal Se.

This comparison is useful in Te where no ring molecules are known to exist, yet experimentally it is found[45] that the dominant Raman peak in a-Te is shifted to much higher frequencies (~150 cm^{-1} compared to 122 cm^{-1} in the trigonal crystal[10,14]). These frequencies in a-Te are apparently higher than any modes of the trigonal crystal.[10] By analogy with Se we make the anzatz that this change is due to the secondary bonding in the crystal. Brodsky *et al.*[45] have also suggested this interpretation. This is further supported by the facts that in a-Te, R/r is much larger[46] than in the crystal as shown in Table II, and the band gap is increased to ~0.8 eV from[47] the value of ~0.35 eV in the crystal, i.e., an increase in the covalent primary bonding in a-Te. In a manner very analogous to Se, we have evaluated K_{rR} by (i) assuming a-Te is made up of isolated chains, (ii) scaling primary constants by $(r_{\text{amorph}}/r_{\text{chain}})^3=(2.79/2.84)^3=0.948$, (iii) assuming K_R is reduced by one-half (the results are insensitive to this particular choice) and $K_{R\Theta}=K_\Theta=K_{rR}=0$ in the amorphous case, and (iv) attributing all remaining discrepancies in the Γ_1 frequency

to K_{rR} in the trigonal form. The resulting value of K_{rR} for the trigonal crystal is given in Table IV. As we found in Sec. IV, this value of K_{rR} improves the description of the upper dispersion curves in Te.

The primary result of the present work applied to the ring and amorphous forms is that no definite aspects of the secondary bonding have been detected. This appears to be both because the forces are much weaker than in the trigonal forms and because their effects are very complex and tend to be averaged out, i.e., there is no single frequency which is particularly sensitive to secondary bonding. The data for the amorphous forms are consistent with the picture of relatively isolated molecular units.

VI. SUMMARY AND CONCLUSIONS

We have shown that from both structural data (Sec. II) and lattice dynamical data (Secs. IV and V) the different forms of Se and Te form a spectrum of materials having varying degrees of molecular character. All ring forms and amorphous forms appear to be essentially molecular, however the trigonal forms of Se and Te have distinct signs of nonmolecular behavior, i.e., strong secondary bonding.

The interatomic forces were described in a valence force field picture with the constants determined by approximate fitting of available frequency data. In addition, algebraic expressions were presented which can be used to calculate frequencies at high-symmetry points for any values of the force constants and for a range of c/a values.

The tendency toward nonmolecular character in the trigonal crystals was cast in the language of a phase transition to a nonmolecular metallic hexagonal structure. The order parameter for the transition was shown to be $(R/r-1)$, where r and R are the primary and secondary bond lengths respectively, and the restoring for this order parameter was shown to be the Γ_1 mode frequency squared.

Chemical bonding arguments supported the existence of driving forces toward the metal-insulator instability and showed that they should be accompanied by noncentral secondary forces. Quantitative calculation of the force constants supported the general picture: (i) Noncentral secondary forces were shown to exist and to increase relative to other forces in going from Se to Te. (ii) Interaction between primary and secondary bonding (K_{rR}) was shown to be consistent with the major features of the lattice vibration spectra of the various forms. (iii) The force constant K_{rR} which increases rapidly with increasing secondary interactions was shown to lead to a natural explanation for the decrease in the Γ_1 optic frequency of the trigonal crystals under pressure.[20]

It would be particularly interesting to explore the pressure dependence of the frequencies for pressures near the actual phase transitions.[4,5] Modes which have not been studied under pressure, for example Γ_2 and the lowest B_2 mode, would provide a better quantitative picture of the change in chemical bonding in this case of a pressure induced insulator-metal transition.

ACKNOWLEDGMENTS

We are grateful for many conversations to H. Bilz, W. Weber, H. Wendel, W. D. Teuchert, W. Richter, T. A. Fjeldly, and R. Zallen, to W. D. Teuchert and H. Wendel for communication of their results prior to publication, and to M. Rodoni and F. E. Kerr for their assistance in this work.

---

*Part of this work was done while one of us (R. M. M.) was a visiting scientist at the Max Planck Institut für Festkörperforschung, Stuttgart 7, West Germany.

[1]L. Pauling, *The Nature of the Chemical Bond* (Cornell U.P., Ithaca, N. Y., 1960).
[2]J. C. Phillips, Rev. Mod. Phys. 42, 317 (1960).
[3]G. S. Pawley and S. J. Cyvin, J. Chem. Phys. 52, 4073 (1970).
[4]D. R. McCann and L. Cartz, J. Chem. Phys. 56, 2552 (1972).
[5]J. C. Jamieson and D. B. McWhan, J. Chem. Phys. 43, 1149 (1965).
[6]R. W. G. Wyckoff, *Crystal Structures* (Interscience, New York, 1951), Vol. 1.
[7]P. Grosse, in *Springer Tracts in Modern Physics*, edited by G. Höhler (Springer Verlag, Berlin, 1969), No. 48.
[8]A. von Hippel, J. Chem. Phys. 16, 372 (1948).
[9]W. Geisler, A. Axmann, and T. Springer, *Neutron Inelastic Scattering* (IAEA, Vienna, 1961), p. 245.
[10]B. M. Powell and P. Martel, in *Proceedings of the Tenth International Conference on the Physics of Semiconductors* (U. S. AEC, Technical Information Div., Oak Ridge, Tenn., 1970), p. 851; J. Phys. Chem. Solids (to be published).
[11]W. C. Hamilton, B. Lassier, and M. I. Kay, J. Phys. Chem. Solids 35, 1089 (1974).
[12]W. D. Teuchert, R. Geick, G. Landwehr, H. Wendel, and W. Weber (unpublished).
[13]G. Lucovsky, R. C. Keezer, and E. Burstein, Solid State Commun. 5, 493 (1967).
[14]A. S. Pine and G. Dresselhaus, Phys. Rev. B 4, 356 (1971).
[15]G. Lucovsky, A. Mooradian, W. Taylor, G. B. Wright, and R. C. Keezer, Solid State Commun. 5, 113 (1967).
[16]G. Lucovsky, in *Physics of Selenium and Tellurium*, edited by W. C. Cooper (Pergamon, Oxford, 1969), p. 255; A. Mooradian and G. B. Wright, *ibid*, p. 269.
[17]G. Lucovsky, Phys. Status Solidi B 49, 633 (1972).

[18]T. A. Fjeldly and W. Richter (unpublished).
[19]L. D. Landau and E. M. Lifshitz, *Statistical Mechanics* (Pergamon, Oxford, 1962).
[20]W. Richter, J. B. Runucci, and M. Cardona, Phys. Status Solidi B 56, 223 (1973).
[21]R. M. Martin and G. Lucovsky, in *Proceedings of the Twelfth International Conference on the Physics of Semiconductors* (Teubner, Stuttgart, 1974), p. 184.
[22]R. M. Martin and G. Lucovsky, Bull. Am. Phys. Soc. 19, 365 (1974).
[23]P. Unger and P. Cherin, in Ref. 16, p. 223.
[24]D. W. Scott, J. P. McCullough, and F. H. Kruse, J. Mol. Spectrosc. 13, 313 (1964).
[25]J. F. Nye, *Physical Properties of Crystals* (Oxford U. P., Oxford, England, 1957), pp. 260–274.
[26]P. Boolchard, B. B. Triplett, S. S. Hanna, and J. P. deNeufville, in *Mössbauer Effect Methodology*, edited by I. J. Gruverman *et al.* (Plenum, New York, 1974), Vol. 9.
[27]A. Koma, O. Mizuno, and S. Tanaka, Phys. Status Solidi B 46, 225 (1971).
[28]H. Krebs, *Fundamentals of Inorganic Crystal Chemistry* (McGraw-Hill, London, 1968), p. 135.
[29]I. Chen, Phys. Rev. B 7, 3672 (1973); S. Tutihasi and I. Chen, Phys. Rev. 158, 623 (1967).
[30]J. D. Joannopoulos, M. Schlüter, and M. L. Cohen, Phys. Rev. B 11, 2186 (1975).
[31]M. J. P. Musgrave and J. A. Pople, Proc. R. Soc. 260, 474 (1962).
[32]H. L. McMurry, A. W. Solbrig, Jr., and J. K. Boyter, J. Phys. Chem. Solids 28, 2359 (1967).
[33]M. Hulin, Ann. Phys. 8, 647 (1963).
[34]R. Geick, U. Schroder, and J. Stuke, Phys. Status Solidi B 24, 99 (1967).
[35]T. Nakayama, Y. Ideda, and A. Odajima, J. Phys. Soc. Jpn. 30, 885 (1971).
[36]T. Nakayama and A. Odajima, J. Phys. Soc. Jpn. 33, 12 (1972).
[37]T. Nakayama and A. Odajima, J. Phys. Soc. Jpn. 34, 732 (1973).
[38]H. Wendel, W. Weber, and W. D. Teuchert (unpublished).
[39]E. R. Cowley, Can. J. Phys. 51, 843 (1973).
[40]I. Chen and R. Zallen, Phys. Rev. 173, 833 (1968).
[41]M. Born and K. Huang, *Dynamical Theory of Crystal Lattices* (Oxford U. P., Oxford, 1954).
[42]Recently Teuchert *et al.* (Ref. 12) have measured the dispersion in the upper optic branches of Se. Their primary result is that there is considerable dispersion in all directions. In particular, the upper Z_3 and B_1 modes have frequencies of ~ 260 cm^{-1}, well above all frequencies at Γ. These data were not used in the present calculations. The calculated dispersion is similar to, but give dispersion considerably smaller than, the experimental results.
[43]From the data of Ref. 16 we have assigned the strongest Raman feature at 256 cm^{-1} to be the A_1 mode, although the authors chose a mode at 251 cm^{-1} to make the order of the modes the same as in S_8.
[44]E. H. Henninger, R. C. Buschert, and L. Heaton, J. Chem. Phys. 46, 586 (1967); R. Kaplow, T. A. Rowe, and B. C. Averbach, Phys. Rev. 168, 1068 (1967).
[45]M. H. Brodsky, R. J. Gambino, J. E. Smith, Jr., and and Y. Yacoby, Phys. Status Solidi B 52, 609 (1972).
[46]T. Ichikawa, Phys. Status Solidi B 56, 707 (1973).
[47]J. Stuke, J. Non-Cryst. Solids 4, 1 (1970).